The Choice of the Exchange-Correlation Functional for the Determination of the Jahn–Teller Parameters by the Density Functional Theory

Ljubica Andjelković,[a] Maja Gruden-Pavlović,[b] Claude Daul,[c] and Matija Zlatar*[a]

The Jahn–Teller (JT) parameters for small, aromatic, organic radicals, C_nH_n (n = 4–7), bis(cyclopentadienyl)cobalt(II) (cobaltocene), a sodium cluster (Na_3), a silver cluster (Ag_3), the hexaflurocuprate(II) ion ($[CuF_6]^{4-}$), and tris(acetylacetonato) manganese(III) ($[Mn(acac)_3]$) have been evaluated by the means of the multideterminantal density functional theory using the most common approximations, to clarify which type of exchange-correlation functional should be used in analysis of the JT effect. The results are compared with available experimental and theoretical data. The choice of the functional strongly depends on the chemical system at hand, but to obtain fast and qualitatively reliable results, the local density approximation may be taken as satisfactory, regardless of the diversity of the systems prone to a JT distortion. © 2012 Wiley Periodicals, Inc.

Introduction

Rapid progress in computational science, combined with advances in a development of the electronic structure theory, made computational chemistry in recent years an inseparable partner to an experiment. Computational chemistry gives not only qualitative insight into chemical phenomena but also can be used as guide experiments, being able to help in the prediction of new materials and chemical processes. From a fundamental point of view, at the same time, it gives insight into the physical origin of the problem. From a broad palette of electronic structure methods, the density functional theory (DFT)[1,2] emerged as one of the mainstream quantum chemical methods, mainly because it gives a good compromise between accuracy of the results and computational economy. DFT is an exact reformulation of many-body quantum mechanics in terms of the electron density rather than the wavefunction. The essence of the DFT is that all the properties of the system can be, at least in principle, calculated from the ground state electron density of the system alone. All the many-body exchange and correlation effects are contained in the exchange-correlation (XC) potential, which should be universal but is, unfortunately, an unknown functional of the density. Thus, in practice, this relatively small term with respect to the other contributions has to be approximated. The accuracy of DFT calculations predominantly depends on the suitability of the approximations made for the XC functional. In contrast to the wavefunction-based methods, DFT lacks a procedure to improve systematically the accuracy, and one of the biggest skills in using DFT to reproduce and predict various properties of molecules is the proper choice of the XC functional. Much of the research in the field of DFT is devoted to develop new XC functionals, which will yield to the results of better quality. Different XC functionals give more or less accurate results for the different problems under study.[3–9] The choice of the XC functional to be used in practice depends primarily on the chemical nature of the system and the problem under study.

Despite the general success of the application of the DFT in a variety of tasks in modern chemistry and physics, there are still some troublesome issues, such as the treatment of excited states, weak interactions, and degenerate states. Substantial progress in dealing with these issues has been made lately.[10] Degeneracy of electronic states is particularly difficult to handle,[11] although it is proved that the DFT can treat degenerate states.[12–17] Degeneracy of the electronic states in molecules gives rise to the Jahn–Teller (JT) effect.[18,19] The JT theorem states that a molecule in a degenerate state is distorted to a point group of lower symmetry, according to the epikernel principle, which lifts the electron degeneracy and lowers the energy. A lot of interesting phenomena are connected with the JT effect, such as high-T_C superconductivity,[20,21] the colossal magnetoresistance in manganites,[22] stereochemistry, reactivity, spectroscopic and magnetic properties of molecules, co-operative phenomena, phase transition and orbital ordering in crystals, single molecular magnets, structure and spectroscopy of impurity centers, conical intersections in photochemistry, and so forth.[19,23,24] The first goal in the analysis of a JT system is the determination of the JT parameters that quantify
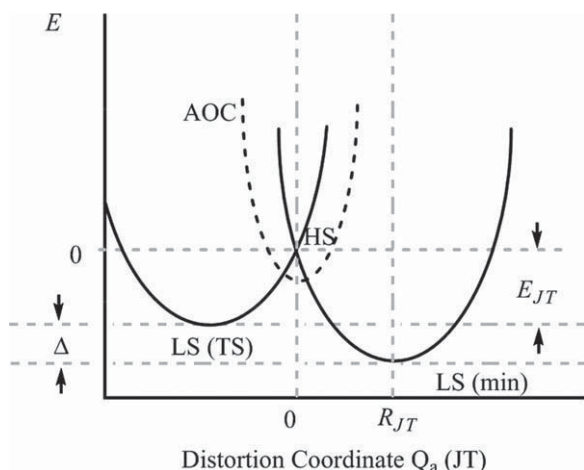
[a] Lj. Andjelković, M. Zlatar
Center for Chemistry, IHTM, University of Belgrade, Studentski trg 12–16, 11000 Belgrade, Serbia
E-mail: matijaz@chem.bg.ac.rs

[b] M. Gruden-Pavlović
Faculty of Chemistry, University of Belgrade, Studentski trg 12–16, 11000 Belgrade, Serbia

[c] C. Daul
Department of Chemistry, University of Fribourg, Chemin du Musée 9, CH-1700 Fribourg, Switzerland

Figure 1. Qualitative cross-section through the potential energy surface, along JT active distortion coordinate Q_a; definition of the JT parameters—the JT stabilization energy, E_{JT}, the warping barrier, Δ, and the JT radius, R_{JT}.

the adiabatic potential energy surface: the JT stabilization energy (E_{JT}), which gives energy stabilization due to the JT effect, the warping barrier (Δ), and the JT radius (R_{JT}), which shows the direction and magnitude of the distortion, Figure 1.

Wavefunction-based methods, such as configuration interaction or complete active space self-consistent field (CASSCF), have been predominantly used for this purpose. All these accurate *ab initio* approaches are very time consuming, especially when a large enough basis set is used to achieve good accuracy, which forbids the treatment of large molecules that may be of a practical interest. Multideterminantal DFT, developed by Daul and coworkers,[25] can be successfully applied in a detailed analysis of JT active molecules, and the results obtained so far are very promising.[26–35]

Bearing in the mind the importance of the proper choice of the XC functional, in this article, the influence of different XC functionals for the analysis of the JT effect by the means of the multideterminantal DFT approach is explored. It is noteworthy that none of the present-day approximate XC functional was constructed to deal with vibronic coupling effects. Herein, the results obtained by the multideterminantal DFT procedure for a series of different JT active molecules: small aromatic organic radicals, organometallic compound, metal clusters, and Werner-type complexes with different XC functionals are presented. There are no guarantees when selecting an XC approximation, but in the following, some general guidelines in the analysis of the JT effect in this simple and efficient way are offered.

Methodology

Multideterminantal DFT method is exhaustively described elsewhere.[25–35] The underlying idea of the practical scheme of this approach is presented in Figure 2. It is necessary to know the geometries and energies of the high symmetry (HS) and low symmetry (LS) points on the adiabatic potential energy surface. This is straightforward for the LS structure. Conversely, the electronic structure of the HS point must be represented by more than one Slater determinant. The use of the average of configuration (AOC) calculation has been proposed to generate the elec-

tron density in the HS point group.[25] This SCF calculation in which the electrons of degenerate orbitals are distributed equally over the components of the degenerate irreps leads to a homogenous distribution of electrons, retains the A_1 symmetry of the total density in the HS point group (step 1). An AOC-type calculation approximates the electronic structure, if the vibronic coupling was not present. Although the AOC gives the proper geometry of the HS species, using simply the energy obtained in this way would be false.[36] Therefore, a single-point calculation imposing the HS on the nuclear geometry and the LS on the electron density was performed (step 2). The last step is straightforward: geometry optimization of the LS structure with different orbital occupations. This yields different LS geometries and energies that correspond to the minimum and to the transition state on the adiabatic potential energy surface, respectively. In summary, the multideterminantal DFT calculation scheme for the particular example of the JT effect in the $[CuF_6]^{4-}$ complex ion, with $t_{2g}^6 e_g^3$ configuration, presented in Figure 2:

1. AOC geometry optimization in O_h (HS) point group with 1.5 electrons placed into each of the two e_{1g} orbitals;
2. Single point calculation with nuclear geometry obtained in step 1, and different D_{4h} (LS) electron distributions, resulting in the energies $E(O_h, {}^2B_{1g})$ and $E(O_h, {}^2A_{1g})$;
3. Geometry optimization in D_{4h} (LS) point group, leading to elongated ($^2B_{1g}$) and compressed ($^2A_{1g}$) structures;
4. The JT stabilization energy, E_{JT}, is the difference between the energies obtained in steps 2 and 3 for the same electron distribution. Difference in energies between the two different LS structures ($^2B_{1g}$ and $^2A_{1g}$) gives the warping barrier, Δ. R_{JT} is given by the length of the distortion vector between the HS and the LS minimum energy configurations.

The DFT calculations were realized using the Amsterdam density functional program package, ADF2010.01.[37–39] Geometry optimization of all the investigated molecules was performed using the local density approximation (LDA) characterized by the Vosko–Willk–Nusair parametrization[40] and a general gradient approximation (GGA), such as Becke-Perdew (BP86),[41,42] Perdew-Wang's gradient correction for exchange
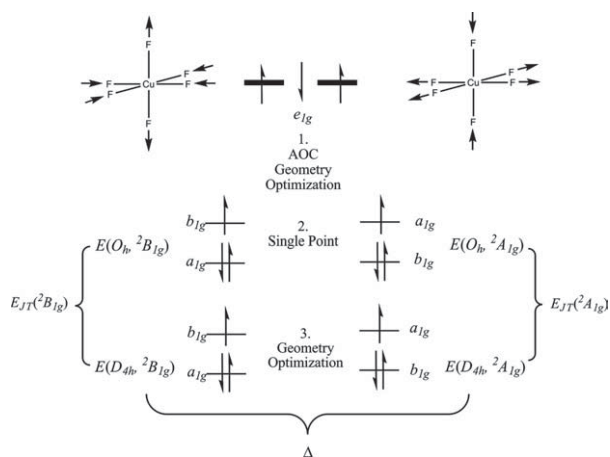
Figure 2. Multideterminantal DFT approach for the calculation of the JT parameters for the $O_h \rightarrow D_{4h}$ distortion of $[CuF_6]^{4-}$.

Table 1. Results of the DFT calculations performed to analyze the JT effect of set of compounds, and compared to reference values; the JT parameters (Figure 1) E_{JT} and Δ are given in cm^{-1} and R_{JT} in (amu)$^{1/2}$ Å.

	Distortion		LDA	BP86	PW91	BLYP	OPBE	B3LYP	Ref
$C_4H_4^{\bullet}$	$D_{4h} \rightarrow D_{2h}$	E_{JT}	2418.2	2469.7	2454.4	2497.1	2413.2	2648.7	2064,[51] 2400,[52] 2250–2637[53]
		Δ	2595.5	2046.2	2096.2	2220.4	1902.7	1842.2	2100[52]
		R_{JT}	0.31	0.32	0.32	0.33	0.31	0.32	–
$C_5H_5^{\bullet}$	$D_{5h} \rightarrow C_{2v}$	E_{JT}	1244.5	1301.8	1294.5	1303.4	1300.2	1685.7	1237[54]
		Δ	0	−0.8	−17.7	−0.8	−1.6	0	–
		R_{JT}	0.25	0.26	0.26	0.27	0.26	0.27	–
$C_6H_6^{+}$	$D_{6h} \rightarrow D_{2h}$	E_{JT}	879.2	884.8	880.0	880.0	891.2	969.5	700–1000[55–57]
		Δ	29.1	−37.1	−31.5	−8.1	−62.9	−39.5	8[58]
		R_{JT}	0.27	0.28	0.28	0.28	0.28	0.28	–
$C_6H_6^{-}$	$D_{6h} \rightarrow D_{2h}$	E_{JT}	788.0	834.0	851.7	856.6	824.3	925.1	–
		Δ	38.7	39.5	54.8	40.3	33.1	17.7	–
		R_{JT}	0.19	0.19	0.19	0.19	0.19	0.29	–
	$D_{6h} \rightarrow C_{2v}$	$E_{PJT/JT}$	1187.3	884.8	949.3	1095.3	887.8	959.0	–
		Δ	46.8	50.8	52.4	42.7	63.5	44.4	–
		$R_{PJT/JT}$	0.62	0.60	0.62	0.60	0.61	0.60	–
$C_7H_7^{\bullet}$	$D_{7h} \rightarrow C_{2v}$	E_{JT}	853.3	922.7	916.3	935.6	917.1	1122.7	1043, 1374[59]
		Δ	0.0	0.0	0.0	0.0	0.0	0.0	–
		R_{JT}	0.16	0.17	0.17	0.17	0.16	0.18	–
$CoCp_2$	$D_{5h} \rightarrow C_{2v}$	E_{JT}	813.8	762.2	761.4	694.4	838.0	727.5	1050[60]
		Δ	0	0	1.6	−0.8	−1.6	−2.4	–
		R_{JT}	0.35	0.34	0.34	0.32	0.35	0.34	–
Na_3	$D_{3h} \rightarrow C_{2v}$	E_{JT}	960.6	1005.8	895.3	1455.8	708.2	1182.4	785,[61] 761,[62] 1160[63]
		Δ	345.2	365.4	300.8	759.8	169.4	450.9	206,[61] 186,[62] 458,[63] 350[19]
		R_{JT}	3.92	4.36	3.68	14.27	2.48	5.49	–
Ag_3	$D_{3h} \rightarrow C_{2v}$	E_{JT}	504.1	685.6	669.4	965.5	805.8	888.8	778,[63] 498[64,65]
		Δ	167.0	289.6	272.6	514.6	345.2	394.4	278,[63] 108[64,65]
		R_{JT}	2.01	3.39	3.19	9.26	4.42	4.97	–
$[CuF_6]^{4-}$	$O_h \rightarrow D_{4h}$	E_{JT}	2417.3	3467.4	2794.7	2917.3	9327.1	2604.4	2083,[66] 2196[67]
		Δ	804.1	1246.1	1117.9	1312.3	7337.3	991.3	–
		R_{JT}	1.89	2.53	1.93	2.74	14.05	2.26	–
$[Mn(acac)_3]$	$D_3 \rightarrow C_2$	E_{JT}	1755.9	1626.0	1619.6	1601.0	842.9	1784.9	1329[68]
		Δ	360.5	325.0	313.8	313.8	424.3	333.9	280[68]
		R_{JT}	1.26	1.44	1.37	1.45	2.06	1.29	–

plus Perdew-Wang's gradient correction for correlation (PW91),[43] Becke-Lee-Yang-Parr (BLYP),[41,44] Handy-Cohen's OPTX correction for exchange plus Perdew-Burke-Ernzerhof's correction for correlation (OPBE),[45] and hybrid Becke 3-Parameter (Exchange), Lee, Yang and Parr (B3LYP).[46,47] An all electron Triple-zeta Slater-type orbitals plus one polarization function basis set was used for all atoms. All calculations were spin-unrestricted. Separation of the orbital and the geometrical symmetry, as used in the calculation of the energies of the HS nuclear configurations (step 2, Fig. 2), is performed using SYMROT sub-block in the QUILD program, version 2010.01,[48] provided in the ADF2010.01 program package. Analytical harmonic frequencies[49,50] were calculated to ascertain whether the LS structures correspond to the stationary points on the adiabatic potential energy surface. Because of the large negative charge of the hexafluorocuprate(II) ion, the conductor-like screening solvation model was included in the DFT calculations,[35] as implemented in ADF, with the dielectric constant of water $\varepsilon = 78.4$.

Results and Discussion

To clarify which XC functional should be used to study the JT effect within a multideterminantal DFT framework, molecules that differ in the nature of chemical bonding, range of E_{JT}, symmetry of distortion, and also type of the JT problem ($E \otimes (b_1 + b_2)$, $E \otimes e$) were chosen. The results for small, aromatic, organic radicals, C_nH_n ($n = 4$–7); an organometallic compound—bis(cyclopentadienyl)cobalt(II) (cobaltocene, $CoCp_2$); small metal clusters—sodium cluster (Na_3) and silver cluster (Ag_3); and Werner-type complexes—hexafluorocuprate(II) ion ($[CuF_6]^{4-}$) and tris(acetylacetonato)manganese(III) ($[Mn(acac)_3]$) are presented in Table 1.

More detailed results for the analyzed molecules are given in Supporting Information Material (Supporting Information Tables S1–S10).

The cyclobutadienyl radical cation ($C_4H_4^{+\bullet}$), the cyclopentadienyl radical ($C_5H_5^{\bullet}$), the benzene cation ($C_6H_6^{+}$), the benzene anion ($C_6H_6^{-}$), and the tropyl radical ($C_7H_7^{\bullet}$) have a single electron or a hole in a doubly degenerate highest occupied molecular orbital, representing the family of JT active hydrocarbon rings. Unlike the $C_5H_5^{\bullet}$, $C_6H_6^{+}$, $C_6H_6^{-}$, and $C_7H_7^{\bullet}$, which are examples of the $E \otimes e$ problem, $C_4H_4^{+\bullet}$ presents a paradigm of $E \otimes (b_1 + b_2)$ JT problems. In all cases, good agreement with both experimental and theoretical data is achieved.[51–59,69–75] It is noteworthy that the experimental determination of the JT parameters is very difficult and there are often uncertainties in the values, because they are obtained from fitting to different models. Conversely, theoretical values fall within a broad range; hence, it is often hard to say which value is the reference one. The previous CASSCF calculation for $C_4H_4^{+\bullet}$ revealed

an E_{JT} of 2637 cm^{-1},[53] which is in agreement with the present results. $C_5H_5^{\bullet}$ is one of the most studied JT active molecules both experimentally and theoretically, and the results obtained by Miller and Applegate who used dispersed fluorescence spectroscopy are considered to be the benchmark result ($E_{JT} = 1237$ cm^{-1}).[54] Multideterminantal DFT calculation at the LDA level of theory gives a value of 1244 cm^{-1}, which is even better than the values obtained by high level *ab initio* calculations. The calculated data for $C_6H_6^+$ are in accordance those of previous theoretical studies, which report values of E_{JT} between 700 and 1000 cm^{-1}.[55–57] The experimentally estimated JT stabilization energy for $C_7H_7^{\bullet}$ is 1043 cm^{-1}, whereas a previously theoretically obtained value is 1374 cm^{-1}.[59] The obtained values for the JT parameters with different XC functionals are consistent (Table 1), except in the case of B3LYP, where an overestimation of E_{JT} can be noticed. This is not surprising, as B3LYP has a tendency to overestimate the exchange and correlation energies of localized electrons.[76] Furthermore, the semiempirical nature of this functional is also a possible source of errors. In the case of $C_6H_6^+$, a change of the XC functional leads to a change in the ground electronic state in the LS point, that is, LDA gives the $^2B_{2g}$ state, whereas GGA and B3LYP give $^2B_{3g}$ as the minimum on the Potential energy surface (PES), Table 1 and Supporting Information Table S3. As the values of the warping barrier are in the range from −39.5 cm^{-1} to 29.1 cm^{-1}, the JT effect can be considered as dynamic, independent of the choice of the XC functional used. The warping barrier is experimentally reported to be 8 cm^{-1}, and the $^2B_{2g}$ state to be the minimum.[58]

Cobaltocene (CoCp$_2$), one more example of the $E \otimes e$ JT problem, possesses two possible HS conformations, eclipsed (D_{5h}) and staggered (D_{5d}). The presented results are limited to CoCp$_2$ in D_{5h} symmetry, as DFT calculation revealed that the eclipsed conformation is more stable and the JT effect does not depend on the rotation of the rings.[29] The results of the multideterminantal DFT procedure performed to analyze the JT effect in CoCp$_2$ are given in Supporting Information (Supporting Information Table S6). Similar to the cases of the organic radicals, the values of the JT parameters in this organometallic compound do not depend significantly on the choice of the XC functional. The different ground states obtained using different functionals (Table 1 and Supporting Information Table S6) are due to the very small warping barriers, which are in the range of the precision of the calculation. The calculated parameters, Table 1, are in agreement with the value of 1050 cm^{-1}, estimated from solid-state Electron Paramagnetic Resonance (EPR) spectra.[60] In contrast to, for example $C_5H_5^{\bullet}$, the experimental value for CoCp$_2$ cannot be considered as a benchmark, as the experimental results are strongly dependent on the diamagnetic host matrix.[60]

The electronic structures of Na$_3$ and Ag$_3$ molecules are determined primarily by the behavior of three valence electrons (one donated by each Na or Ag atom). In the HS, D_{3h} point group, sodium and silver clusters indicate to the existence of degenerate electronic states. The JT distortion leads to a splitting of the degenerate state $^2E_1'$ into $^2A_1$ and $^2B_2$ with a descent in symmetry to C_{2v}. According to the DFT calculations, the $^2B_2$ state represents the global minimum, while the transition state on the potential energy surface is $^2A_1$. Analyzing the influence of different XC functionals for Na$_3$ and Ag$_3$ clusters revealed that BLYP approximation overestimates the JT stabilization energy, the warping barrier and the JT radius, Table 1, and the geometry differs significantly. The DFT results at the BLYP level give one bond length to be 6.5 Å and other two 3.3 Å and one angle with the value of 164.5° and other two 7.3°, which are far removed from the results obtained with the other applied XC approximations and the reference values.[61] The same trend was observed for the Ag$_3$ molecule. Hence, the BLYP is shown to be less accurate than the other applied XC functionals. In both cases, good agreement with previous theoretical studies is obtained,[19,61–65,77,78] with the exception of the aforementioned BLYP (Table 1, Supporting Information Tables S7 and S8).

It is a well-known fact of coordination chemistry that hexacoordinated copper(II) and manganese(III) complexes exhibit a strong JT coupling. In the O_h point, the copper(II) ion has a ^2E_g electronic ground state. After descent in symmetry to D_{4h}, the electronic state splits into $^2A_{1g}$ and $^2B_{1g}$, compressed and elongated geometry, respectively. The results for the JT parameters are presented in Table 1 and Supporting Information Table S9. The values for the warping barrier, Δ, unambiguously indicate that the adiabatic potential energy surface is not flat, thus the state $^2B_{1g}$ belongs to the energy minimum, whereas $^2A_{1g}$ is the transition state. The octahedral Cu(II) units in the crystals of K$_2$CuF$_4$, Ba$_2$CuF$_6$, and so forth, were originally misinterpreted as compressed by EPR measurements and X-ray data. More elaborate investigations, including Extended X-Ray Absorption Fine Structure (EXAFS) measurements, showed that, in fact, the local octahedra are elongated.[79–81] The evaluated E_{JT} values are in the range 2400–3400 cm^{-1} for all used functionals, with the exception of OPBE, which gives a very high JT stabilization energy. Experimentally estimated E_{JT} values from UV–Vis spectra are found to be 2082.5 or 2195.5 cm^{-1}.[66,67] Thus, to explain the differences in R_{JT}, the bond distances in [CuF$_6$]$^{4-}$ at HS and LS nuclear configurations were analyzed and then compared with the available experimental data, Table 2.[82,83] It can be clearly seen (Table 2) that the

Table 2. Calculated DFT and experimental bond lengths (Å) in [CuF$_6$]$^{4-}$.

[CuF$_6$]$^{4-}$	LDA	BP86	PW91	BLYP	OPBE	B3LYP	EXP[82]	EXP[83]
O_h, Cu-F	2.01	2.10	2.10	2.10	2.12	2.10	2.02	2.05
D_{4h}, ax-Cu-F	2.28	2.45	2.44	2.51	4.37	2.40	2.22	2.30
D_{4h}, eq-Cu-F	1.91	1.96	1.96	1.97	1.93	1.96	1.92	1.93

LDA gives the most accurate geometry. The OPBE gives quite good results for the equatorial bonds in the D_{4h} global minimum structure with absolute deviations from experimental data of 0 Å. However, the axial bond distances are too long (≈ 4.4 Å), indicating the great discrepancy. Other GGA functionals as well as B3LYP show bigger deviation in the observed equatorial bond distances and more accurate results for bond lengths in the axial position.

The other Werner-type complex, [Mn(acac)$_3$], has D_3 symmetry with a $^2E_1$ ground state. Because of the JT effect, the symmetry

4

decreases to C_2, whereby the ground state splits into ^2A and ^2B. An axial elongation corresponds to the ^2A state, the minimum on the potential energy surface, while the transition state, compressed octahedron, is in the ^2B electronic state, higher in energy by 313–425 cm^{-1} (Table 1 and Supporting Information Table S10), which is in good agreement with a previous DFT study.[68] The DFT calculations at the OPBE level clearly underestimate the JT stabilization energies (Table 1 and Supporting Information Table S10). The differences in the values of the JT parameters can be explained by the differences in the geometries obtained with the different level of theory. It is well known that inclusion of gradient corrections leads to bond elongation compared to the LDA results. The overlays of the crystal structure[84] and structures computed at the LDA and OPBE levels are pre-
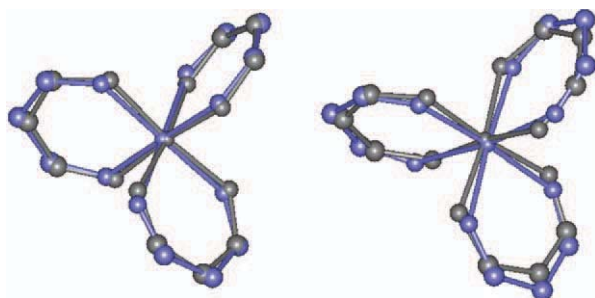
Figure 3. Overlay of experimental X-ray (gray) with LDA-optimized (light blue) global minimum structure (left) and OPBE-optimized (light blue) global minimum structure (right). [Color figure can be viewed in the online issue, which is available at wileyonlinelibrary.com.]

sented in Figure 3. Obviously, the structure obtained with LDA matches better the X-ray structure, which is a confirmation that the LDA tends to give better geometries for Werner-type complexes.[8,32] Therefore, the proper determination of geometry not only in a metric data but also in the conformation of the ligands is very important in the determination of JT parameters.

Conclusions

All molecules under study belong to the JT active species, and they represent completely different chemical systems; hence, the obtained results can be assumed as general.

For small, aromatic, organic radicals and cobaltocene, the JT parameters do not depend on a choice of the XC functional. The results obtained by means of multideterminantal DFT are mutually consistent, regardless of the level of theory, and are in good agreement with the results of previous studies, both experimental and theoretical.

DFT analysis of the JT effect in small metal clusters gives acceptable results for all applied XC functionals, except for BLYP. Thus, one should be careful in using BLYP for the quantification of the JT distortion in such cases.

The LDA tends to give better geometries for Werner compounds in comparison to the GGA and hybrid functionals. The GGA functionals always yield longer bonds and, hence, worse agreement with experimental data for Werner species. Thus, great attention should be given to the choice of the XC functional for the analysis of the JT effect and determination of the

JT parameters in Werner-type complexes. To obtain reliable results, the LDA performs remarkably well, as it provides the best geometries for both the HS and LS species.

The difficulties in the determination of the JT parameters are not to be found in the definition of degenerate states, but in the determination of the precise geometry of the HS and LS points. The JT distortion is a consequence of electronic factors, but strongly depends on the geometry. The selection of the XC functional is strictly connected to the chemical system at hand, but to obtain qualitatively reliable results, the simplest LDA is satisfactory, regardless of the diversity of the systems prone to JT distortion. Although other XC functionals perform better in the quantification of other properties of molecules, that is, B3LYP for magnetic couplings,[4] BP86 for EPR hyperfine data,[5] OPBE for reliable spin-state energies for iron complexes,[6] the LDA appears to be the most accurate for the determination of JT parameters by the means of multideterminantal DFT. Quantification of the JT distortion in this simple and efficient way is of great interest as the experimental determination of the JT parameters is very difficult and there is often uncertainty in the obtained values. Conversely, multireference wavefunction methods are usually not affordable for large systems, giving the advantage to multideterminantal DFT as a reliable tool for the study of vibronic coupling.

[1] R. G. Parr, W. Yang, Density-Functional Theory of Atoms and Molecules; Oxford University Press, New York, USA, **1989**.

[2] R. M. Dreizler, E. K. U. Gross, Density Functinal Theory: An Approach to Quantum Many-Body Problem; Springer-Verlag: Berlin, Heidelberg, New York, London, Paris, Tokyo, Hong Kong, Barcelona, **1990**.

[3] S. F. Sousa, P. A. Fernandes, M. J. Ramos, *J. Phys. Chem. A* **2007**, *111*, 10439.

[4] A. Rodríguez-Fortea, P. Alemany, S. Alvarez, E. Ruiz, *Inorg. Chem.* **2002**, *41*, 3769.

[5] S. Kababya, J. Nelson, C. Calle, F. Neese, D. Goldfarb, *J. Am. Chem. Soc.* **2006**, *128*, 2017.

[6] M. Swart, *J. Chem. Theory Comput.* **2008**, *4*, 2057.

[7] D. Rapport, N. R. M. Crawford, F. Furche, K. Burke, In Computational Inorganic and Bioinorganic Chemistry; E. I. Solomon, R. B. King, Scott R. A., Eds.; Willey, New York, USA, **2009**; pp. 159–172.

[8] M. R. Bray, R. J. Deeth, V. J. Paget, P. D. Sheen, *Int. J. Quantum Chem.* **1996**, *61*, 85.

[9] N. I. Gidopoulos, P. G. Papaconstantinou, E. K. U. Gross, *Phys. Rev. Lett.* **2002**, *88,* 033003.

[10] A. J. Cohen, P. Mori-Sánchez, W. Yang, *Chem. Rev.* **2012**, *112,* 289.

[11] I. B. Bersuker, *J. Comput. Chem.* **1997**, *18,* 260.

[12] M. Levy, *Int. J. Quantum Chem.* **2010**, *110,* 3140.

[13] A. K. Theophilou, *J. Phys. C* **1979**, *12,* 5419.

[14] A. K. Theophilou, P. Papaconstantinou, *Phys. Rev. A* **2000**, *61,* 022502.

[15] E. K. U. Gross, L. N. Oliveira, W. Kohn, *Phys. Rev. A* **1988**, *37,* 2805.

[16] E. K. U. Gross, L. N. Oliveira, W. Kohn, *Phys. Rev. A* **1988**, *37,* 2809.

[17] L. N. Oliveira, E. K. U. Gross, W. Kohn, *Phys. Rev. A* **1988**, *37,* 2821.

[18] H. A. Jahn, E. Teller, *Proc. R. Soc. London, Ser. A* **1937**, *161,* 220.

[19] I. B. Bersuker, The Jahn-Teller Effect; Cambridge University Press, Cambridge, UK, **200**6.

[20] J. G. Bednorz, K. A. Müler, *Z. Phys. B: Condens. Matter* **1986**, *64,* 189.

[21] J. G. Bednorz, K. A. Müler, In Nobel Lectures: Physics 1981–1990; Ekspang, G., Ed.; World Scientific Publishing Co.: Singapore, **1993**; pp. 424–457.

[22] A. J. Millis, *Nature* **1998**, *392,* 147.

[23] I. B. Bersuker, Electronic Structure and Properties of Transition Metal Compounds; Wiley, New York, USA, **2010**.

[24] R. G. Pearson, Symmetry Rules for Chemical reactions; Wiley-Interscience Publication, New York, USA, **1976**.

[25] R. Bruyndonckx, C. Daul, P. T. Manoharan, E. Deiss, *Inorg. Chem.* **1997**, *36,* 4251.

[26] D. Reinen, M. Atanasov, W. Z. Massa, *Anorg. Allg. Chem.* **2006**, *632,* 1375.

[27] M. Zlatar, C.-W. Schläpfer, C. Daul, In The Jahn-Teller-Effect Fundamentals and Implications for Physics and Chemistry; H. Koeppel, D. R. Yarkoni, H. Barentzen, Eds., Vol. *97, Chapter 1; Springer Series in Chemical Physics,* Berlin, Germany, **2009**; pp. 131–165.

[28] M. Zlatar, M. Gruden-Pavlović, C.-W. Schläpfer, C. Daul, *J. Mol. Struct. THEOCHEM* **2010**, *954,* 86.

[29] M. Zlatar, C.-W. Schläpfer, E. P. Fowe, C. Daul, *Pure Appl. Chem.* **2009**, *81,* 1397.

[30] M. Gruden-Pavlović, M. Zlatar, C.-W. Schläpfer, C. Daul, *J. Mol. Struct. THEOCHEM* **2010**, *954,* 80.

[31] M. Zlatar, M. Gruden-Pavlović, C.-W. Schläpfer, C. Daul, *Chimia* **2010**, *64,* 161.

[32] T. K. Kundu, R. Bruyndonckx, C. Daul, P. T. Manoharan, *Inorg. Chem.* **1999**, *38,* 3931.

[33] M. Atanasov, P. Comba, *J. Mol. Struct.* **2007**, *38,* 157.

[34] M. Atanasov, P. Comba, C. A. Daul, A. Hauser, *J. Phys. Chem. A* **2007**, *38,* 9145.

[35] D. Reinen, M. Atanasov, P. Köhler, D. Babel, *Coord. Chem. Rev.* **2010**, *254,* 2703.

[36] Y. Zhang, W. Yang, *J. Chem. Phys.* **1998**, *109,* 2604.

[37] ADF2010.01. SCM, Theoretical Chemistry; Vrije Universiteit Amsterdam: The Netherlands, **2010**, Available at: http://www.scm.com.

[38] C. F. Guerra, J. G. Snijders, G. te Velde, E. J. Baerends, *Theor. Chem. Acc.* **1998**, *99,* 391.

[39] G. te Velde, F. M. Bickelhaupt, S. J. A. van Gisbergen, C. F. Guerra, E. J. Baerends, J. G. Snijders, T. Ziegler, *J. Comput. Chem.* **2001**, *22,* 931.

[40] S. Vosko, L. Wilk, M. Nusair, *Can. J. Phys.* **1980**, *58,* 1200.

[41] A. D. Becke, *Phys. Rev. A* **1988**, *38,* 3098.

[42] J. P. Perdew, *Phys. Rev. B* **1986**, *33,* 8822.

[43] J. P. Perdew, J. A. Chevary, S. H. Vosko, K. A. Jackson, M. R. Pederson, D. J. Sing, C. Fiolhais, *Phys. Rev. B* **1992**, *46,* 6671.

[44] C. Lee, W. Yang, R.G. Parr, *Phys. Rev. B* **1988**, *37,* 785.

[45] M. Swart, A. W. Ehlers, K. Lammertsma, *Mol. Phys.* **2004**, *102,* 2467.

[46] A. D. Becke, *J. Chem. Phys.* **1993**, *98,* 5648.

[47] P. J. Stephens, F. J. Devlin, C. F. Chabalowski, M. J. Frisch, *J. Phys. Chem.* **1994**, *98,* 11623.

[48] M. Swart, F. M. Bickelhaupt, *J. Comput. Chem.* **2007**, *29,* 724.

[49] A. Bérces, R. M. Dickson, L. Fan, H. Jacobsen, D. Swerhone, T. Ziegler, *Comput. Phys. Commun.* **1997**, *100,* 247.

[50] H. Jacobsen, A. Bérces, D. Swerhone, T. Ziegler, *Comput. Phys. Commun.* **1997**, *100,* 263.

[51] M. Roeselová, T. Bally, P. Jungwirth, P. Čársky, *Chem. Phys. Lett.* **1995**, *234,* 395.

[52] W. T. Borden, E. R. Davidson, D. Feller, *J. Am. Chem. Soc.* **1981**, *103,* 5725.

[53] S. Saddique, G. A. Worth, *Chem. Phys.* **2006**, *329,* 99.

[54] B. E. Applegate, T. A. Miller, *J. Chem. Phys.* **2001**, *114,* 4855.

[55] B. E. Applegate, T. A. Miller, *J. Chem. Phys.* **2002**, *117,* 10654.

[56] V. Perebeinos, P. B. Allen, M. Pederson, *Phys. Rev. A* **2005**, *72,* 012501.

[57] K. Tokunaga, T. Sato, K. Tanaka, *J. Chem. Phys.* **2006**, *124,* 154303.

[58] R. Lindner, K. Müller-Dethlefs, E. Wedum, K. Haber, E. R. Grant, *Science* **1996**, *271,* 1698.

[59] I. Sioutis, V. L. Stakhursky, G. Tarczay, T. A. Miller, *J. Chem. Phys.* **2008**, *128,* 084311.

[60] J. H. Ammeter, L. Zoller, J. Bachmann, P. Baltzer, E. R. Bucher, E. Deiss, *Helv. Chim. Acta* **1981**, *64,* 1063.

[61] H. von Busch, V. Dev, H.-A. Eckel, S. Kasahara, J. Wang, W. Demtröder, P. Sebald, W. Meyer, *Phys. Rev. Lett.* **1998**, *81,* 4584.

[62] J. Gaus, K. Kobe, V. Bonačić-Koutecký, H. Kühling, J. Manz, B. Reischl, S. Rutz, E. Schreiber, L. Wöste, *J. Phys. Chem.* **1993**, *97,* 12509.

[63] P. García-Fernández, I. B. Bersuker, J. A. Aramburu, M. T. Barriuso, M. Moreno, *Phys. Rev. B* **2005**, *71,* 184117.

[64] S. P. Walch, C. W. Bauschlicher, S. R. Langhoff, *J. Chem. Phys.* **1986**, *85,* 5900.

[65] K. Balasubramanian, M. Z. Liao, *Chem. Phys.* **1988**, *127,* 313.

[66] M. J. Riley, L. Dubicki, G. Moran, E. R. Krausz, I. Yamada, *Inorg. Chem.* **1990**, *29,* 1614.

[67] W. Kleemann, Y. Farge, *J. Phys. (Paris) Lett.* **1974**, *35,* 135.

[68] I. Diaz-Acosta, J. Baker, J. F. Hinton, P. Pulay, *Spectrochim. Acta Part A* **2003**, *59,* 363.

[69] B. E. Applegate, J. Bezant, T. A. Miller, *J. Chem. Phys.* **2001**, *114,* 4869.

[70] S. Zilberg, Y. Haas, *J. Am. Chem. Soc.* **2002**, *124,* 10683.

[71] T. Sato, K. Tanaka, K. Tokunaga, *J. Chem. Phys.* **2006**, *124,* 024314.

[72] H. J. Silverstone, D. E. Wood, H. M. McConnell, *J. Chem. Phys.* **1964**, *41,* 2311.

[73] R. F. Gunion, M. Karney, P. G. Wenthold, W. T. Borden, W. C. Lineberger, *J. Am. Chem. Soc.* **1996**, *118, 5074.*

[74] E. P. F. Lee, T. G. Wright, *J. Phys. Chem. A* **1998**, *102,* 4007.

[75] T. Pino, F. Güthe, H. Ding, J. P. Maier, *J. Phys. Chem. A* **2002**, *106,* 10022.

[76] J. Paier, M. Marsman, G. Kresse, *J. Chem. Phys.* **2007**, *127,* 024103.

[77] J. A. Howard, R. Sutcliffe, B. Mile, *Surf. Sci.* **1985**, *156,* 214.

[78] J. A. Howard, K. F. Preston, B. Mile, *J. Am. Chem. Soc.* **1981**, *103,* 6226.

[79] H. Stratemeier, B. Wagner, E. R. Krausz, R. Linder, H.-H. Schmidtke, J. Pebler, W. E. Hatfield, L. ter Haar, D. Reinen, M. A. Hitchman, *Inorg. Chem.* **1994**, *33,* 2320.

[80] P. J. Ellis, H. C. Freeman, M. A. Hitchman, D. Reinen, B. Wagner, *Inorg. Chem.* **1994**, *33,* 1249.

[81] D. Reinen, M. A. Hitchman, *Z. Physik. Chem.* **1997**, *200,* 11.

[82] R. Haegele, D. Babel, *Z. Anorg. Allg. Chem.* **1974**, *409,* 11.

[83] W. Massa, D. Babel, *Chem. Rev.* **1988**, *88,* 275.

[84] B. R. Stults, R. S. Marianelli, V. W. Day, *Inorg. Chem.* **1979**, *18,* 1853.